ELSEVIER

Contents lists available at ScienceDirect

# Smart Agricultural Technology

journal homepage: www.journals.elsevier.com/smart-agricultural-technology



# Multimodal sensing approach using remote and onsite data for estimating the pre-harvest ripening stage of Hass Avocado with machine learning algorithms

Nuria López-Ruiz a,b,†,\* , Silvia Prieto-Sánchez c,†, Celia E. Ramos-Lorente b, Alejandro Fernández-Moreno , Antonio J. Pérez-Ávila , David Álvarez-León b, Isabel M. Pérez de Vargas-Sansalvador b,c , Alexander García-Cardenas , Beatriz Molina-García , Alberto J. Palma a,b , Luis F. Capitán-Vallvey b,c , Antonio Martínez-Olmos a,b , Miguel M. Erenas b,c

## ARTICLE INFO

#### Keywords: Multispectral information Machine learning Avocado ripening ANN

#### ABSTRACT

In recent years, avocado has gained significant global importance due to its nutritional benefits, and rising consumer demand, becoming a staple in health-conscious diets. This growing interest has also raised concerns about environmental sustainability, and as a result, efforts are being made to promote more sustainable farming practices while meeting the rising demand. In this study, we present a tool designed to enhance the efficiency of the pre-harvest process and improve avocado quality. We propose a multimodal sensing scheme integrating three different data sources: a portable multispectral system for in situ measurements, satellite imagery and, onsite environmental sensors to estimate the fruit ripening stage. This combined remote and onsite yielded a high correlation with dry matter content, considered here as the reference indicator of avocado ripening, across three consecutive harvest seasons. The performance of various machine learning techniques was evaluated using different combinations of these datasets. Notably, the artificial neural network (ANN) model achieved the highest accuracy (0.74) and recall (0.96) for predicting the overripe avocado class. Therefore, ANN model was extended to regression models, where all of them have demonstrated high predictive accuracy, with R<sup>2</sup> coefficient ranges from 0.81 to 0.91. The online data achieved the highest coefficient (0.91), providing a slightly better performance compared to the offline model. Nonetheless, predictions based solely on multispectral data remain valuable, particularly when online data are unavailable.

# 1. Introduction

Avocado (Persea Americana) contains vitamins A, B, C, E, and K, including 25 essential nutrients. It also contains phytochemicals, like beta-sitosterol, and antioxidants, like lycopene and beta-carotene with proven benefits for a healthy diet [1]. These essential nutrients are

boosting the demand for the fruit globally. The increased demand across the globe has resulted in increased production. According to [2], avocado production was +9.5 million avocados in 2022, which increased by 9.7% and reached 10.4 million in 2023. The avocado market is projected to register a compound annual growth rate (CAGR) of 9.70% from 2024 to 2031 [3]. Avocados, as a climacteric fruit, can be picked

<sup>&</sup>lt;sup>a</sup> Electronic and Chemical Sensing Solutions (ECsens), CITIC-UGR, iMUDS, Department of Electronics and Computer Technology, University of Granada (UGR), Granada 18014, Spain

<sup>&</sup>lt;sup>b</sup> Unit of Excellence in Chemistry Applied to Biomedicine and the Environment of the University of Granada, Granada, Spain

c Fundación I+D del Software Libre (Fidesol), Armilla 18100, Granada, Spain

d ECsens, Department of Analytical Chemistry, University of Granada, Granada 18071, Spain

<sup>&</sup>lt;sup>e</sup> Grupo Empresarial La Caña SL, Cortijo El Rancho, s/n, Gualchos 18740, Granada, Spain

<sup>\*</sup> Corresponding author at: Electronic and Chemical Sensing Solutions (ECsens), CITIC-UGR, iMUDS, Department of Electronics and Computer Technology, University of Granada (UGR), Granada 18014, Spain.

E-mail address: nurilr@ugr.es (N. López-Ruiz).

<sup>†</sup> Both authors contributed equally to this work.

mature but still unripe, continuing the ripening process after the harvesting [1,4]. However, they can also remain on the tree as long as needed, depending on market conditions. However, leaving them too much time on the tree will cause an over-mature state that will lead the fruit to short shelf life and other problems after the harvest, causing huge economic losses [5]. Moreover, given their high perishability, avocados require timely and well-coordinated harvesting and post-harvest handling, and uninterrupted cold chains. An important determining factor of the external and internal eating quality of ripe avocado fruit quality is maturity level at harvest. Therefore, the determination of the avocado maturity stage on the tree is quite relevant to guarantee an optimum state before harvesting. When avocados are harvested from the tree, a fast-ripening process takes place: 12–18 days of external colour changes and a loss of firmness are clear indicators of the avocado ripening [6].

Several parameters provide non-visual, informative indicators related to avocado ripening that could facilitate direct assessment on the tree (pre-harvest): moisture content, mesocarp oil or dry matter, among others. However, most of them are still determined using invasive techniques. Both avocado mesocarp oil content and dry matter gradually increase during fruit growth and exhibit strong correlations with maturity and eating quality [7]. In fact, mesocarp oil content along with related attributes such as dry matter and moisture contents are globally accepted as reliable maturity indices for determining optimal harvest timing [8–10]. In the Tropical Coast (Spain) avocado dry matter typically ranges from 21 % at the onset of the season (October) to around 31 % when the avocado is considered to be optimal for consumption (January). Firmness is also a significant parameter to determine the maturity stage of harvested avocados, and numerous studies for non-destructive estimation of firmness have been reported [5,11–14].

Due to their non-destructive nature, there is increasing interest in implementing non-invasive techniques such as spectroscopic, image processing or acoustic methods [15] to assess avocado ripening and quality. Several studies have been carried out to study the maturity stage through image analysis, as these approaches avoid the human subjectivity of manual analysis, they are usually cheaper than other techniques, and they can easily provide in-situ results [16-18]. In this context, the use of colorimetric parameters obtained from colorimeters/spectrometers [19,20], cameras [21] or smartphones [22] as analytical devices for evaluating external appearance have demonstrated promising results. Some researchers have tried to determine dry matter of the avocado using near-infrared spectroscopy (NIR) [23,24] and even using portable instrumentation [25]. Recently, low-cost multispectral prototypes for fruit ripening assessment of fruits have been developed [26,27]. However, to date, none have conducted comparative analysis of machine learning models including consecutive crops, nor have they systematically compared various regression and classification methodologies

A comprehensive review of various invasive and non-invasive techniques for the determination of avocado maturity stage is presented in [28]. However, the correlation between dry matter content and multispectral data for predicting the optimal maturity state of avocados remains unexplored. Most published studies focus on the information obtained during the post-harvest storage, causing high variation in product quality and posing challenges for harvest scheduling. Visible/NIR multispectral sensors can only gather a limited number of spectral bands, requiring the use of machine learning algorithms or multivariable correlation techniques to relate this information to maturity parameters such as dry matter content of firmness [24,29-34]. Moreover, spectral shape features, described by specific spectral indices, are shown to enhance the interpretability and predictive power of the spectral data [32]. Meanwhile, satellite imagery has recently been integrated with machine learning approaches for crop monitoring applications, including fruit yield estimation in mango [35], avocado orchards [36], and rice grain moisture content [37]. Nonetheless, relying on a single data source may impose inherent limitations. To address these constraints, multimodal sensing strategies, where data from multiple sources are combined, have been increasingly adopted to improve predictive performance and robustness [38,39].

Hence, this work aims to correlate the dry matter content (considered the reference indicator of ripeness) in pre-harvest avocados with a multimodal sensing framework throughout the entire harvesting period. This multimodal scheme integrates remote data, including satellite imagery and onsite environmental sensors measurements, with fruit-level data obtained via a custom-developed multispectral system. The latter acquires diffuse reflectance measurements of avocados using the developed multispectral sensor described in [40]. We propose an offline model using only onsite multispectral data, making it suitable for field applications where internet connectivity is limited or unavailable. In contrast, the online model incorporated additional data sources, including satellite-derived indices and environmental data collected on the farm. To our knowledge, this is the first study to combine offline/online and onsite/remote data sources for fruit ripening assessment. Various machine learning techniques (classification and regression models) were applied and evaluated across all possible dataset combinations. These results will potentially help to enhance pre-harvest decision-making efficiency, improve avocado quality at retail outlets, and reduce post-harvest losses within the agri-food supply chain. Although the experiment was conducted in a controlled environment (Fig. 1), the techniques and methodologies employed can be readily adapted for field deployment in a smartphone-based prototype. Such a device would integrate the trained model, include a physical enclosure to shield the sensor from ambient lighting variations, and implement a light correction algorithm to ensure consistent data quality under varying field conditions [42].

# 2. Material and methods

# 2.1. Collection and preparation of samples

Hass avocado fruits were picked from a commercial orchard located in Motril, Province of Granada, Spain, specifically from designated sectors 1 and 4. Sampling was conducted weekly throughout three consecutive harvest seasons periods, from September to February from 2020 to 2023. Ten trees of Hass variety of avocado exhibiting similar growth stages were randomly selected as sampling sites. A total of 476 avocados were collected over the 2020-2021, 2021-2022 and 2022-2023 seasons, comprising 110, 220 and 146 avocados, respectively. To maintain consistency, fruits of comparable size were selected, and measures were taken to minimize thermal exposure during transportation and storage. Given the study's focus on the pre-harvest ripening process, all measurements using the developed multispectral system were conducted within 24 h of harvest, preserving the avocados in low temperature conditions. In the laboratory, each fruit was assigned a unique identifier, weighted, and photographed to ensure an appropriate register of each sample.

# 2.2. Multispectral system description and data acquisition

Multispectral data were acquired adapting a previously developed portable multispectral system [40]. The instrument is depicted in Fig. 1. Electronic components are enclosed in a black box of  $9\times15\times3$  cm³, and inside, the printed circuit board has dimensions of  $8\times12$  cm², being the main block, the sensing module. This block consists of a light-emitting diode (LED) array distributed in a squared pattern, as a multispectral source, surrounding a digital colour sensor acting as the reflectance detector. For UV/VIS/NIR optical excitation, the ten selected LED models are shown in Table 1.

To achieve a more uniform irradiance pattern over the sample, two LEDs of each wavelength were included, disposed in symmetrical position regarding the colour detector which is placed in the centre of the square. The S11059–02DT (Hamamatsu Photonics K.K. Japan) colour

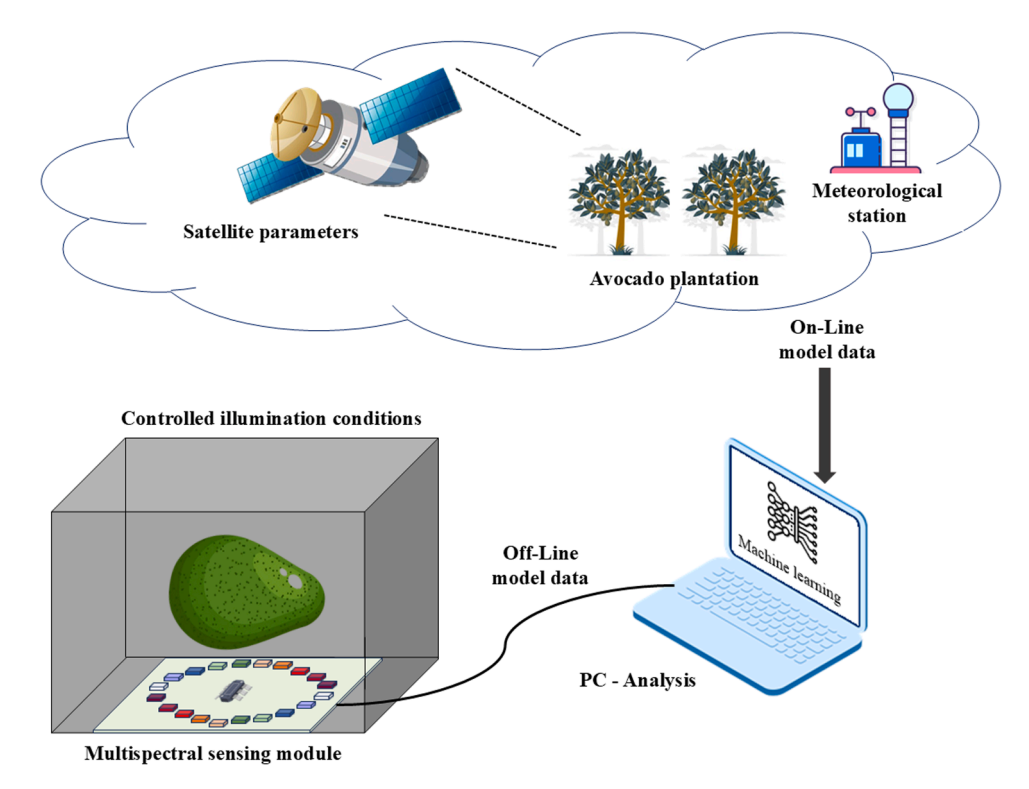


Fig. 1. Experimental setup holding the multispectral system in a black case in order to obtain the measurements avoiding external light influence.

**Table 1**LEDs for multispectral optical excitation.

LED Reference	Manufacturer	λpeak (nm)
SML-LX2832UWC- TR	Lumex Inc., Carol Stream, IL, USA	White clear
VLMU3100	Vishay Intertechnology Inc., Malvern, PA, USA	405
LD MSVG-JGLH- 46–1	OSRAM Opto Semiconductors GmbH, Germany	455
AA3021ZGSK APTR3216PGW APT2012NW APT2012SRCPRV	Kingbright Electronic Co., Ltd., New Taipei City, Taiwan	515 555 610 655
SML-LX15HC-RP-TR	Lumex Inc., Carol Stream, IL, USA	700
VSMG2700 VSMF3710	Vishay Intertechnology Inc., Malvern, PA, USA	830 890

detector used is an I2C interface-compatible model that allows to choose the sensitivity mode as well as the integration time during which the reflected light is collected. In a high sensitivity mode, the photosensitive area of the colour detector is  $0.56 \times 1.22 \text{ mm}^2$ . It is sensitive to four different bands: red (575 to 660 nm,  $\lambda_{peak} = 615$  nm), green (455 to 630 nm,  $\lambda_{peak} = 530$  nm), blue (400 to 540 nm,  $\lambda_{peak} = 460$  nm), and near infrared (700 to 885 nm,  $\lambda_{\text{peak}} = 855$  nm) radiations. Therefore, for each excitation LED, four data are acquired: xxx\_r, xxx\_g, xxx\_b, and xxx\_ir, where xxx refers to white or the maximum emission of each LED and r,g, b,ir to the red, green, blue and infrared detector output channels respectively. During the system operation, each pair of LEDs with the same emission spectra are sequentially activated, and the received light is codified into words of 16 bits of resolution. To obtain a similar response of the system for each LED source, the integration time parameter was individually configured, ranging from 175 ms to 1.75 s. The colour sensor is facing an aperture in the black box, where the sample is placed. As mentioned, RGB and infrared (IR) coordinates are measured and sent to a microcontroller for further processing. More

details can be read elsewhere [40].

Spectral data were acquired from four orthogonal positions along its equatorial contour with the multispectral device as shown in Fig. 1. The fruit was placed in the instrument over a black foam for a better fit of the fruit irregular surface. The analysis was carried out in dark conditions in order to avoid external light influence on the results. Three replicas were captured for each position, having a total of twelve multispectral measurements for each analysed avocado. The dataset was generated by averaging multispectral measurement for each fruit at each spectral band and LED. Each avocado sample was associated with both its respective measured dry matter content, detailed below, and its harvest date.

# 2.3. Environmental and satellite data

As an important novelty in this work, some environmental parameters and satellite imagery data were also measured at the moment of harvesting and included in the classification analysis. Regarding the environmental sensor data, the avocado farm has installed several sensors that gather specific variables for integration into the predictive model. These variables include surface and deep tension (DT), soil humidity (RHS), vapour pressure deficit (VPD), ambient temperature (TA) and soil temperature (TS). These variables were collected using a climate data access API at intervals of approximately 10-15 min. The data collected by the sensors were organised into consecutive subsets, known as 'temporal windows'. These 'windows' were created by segmenting the dataset at regular time intervals. Specifically, each 'window' encapsulated 100 sequential measurements of the 5 variables, consequently with a duration between 16 and 25 h. Within each window, the corresponding output or dry matter value was determined by selecting the measurement closest in time to the end of the window. This approach ensured that the value used for the output within each window corresponded to the most recent measurement in relation to the window's end time.

In addition, satellite Sentinel 2 (Copernicus Sentinel Missions, ESA, EU) images from the periods corresponding to avocado harvests were

employed to compute the Normalised Difference Vegetation Index (NDVI) and the Normalised Difference Red Edge Index (NDRE) for specific sectors within the estate where the fruits were collected. NDVI measures the greenness, and the density of the vegetation captured in a satellite image. Healthy vegetation has a very characteristic spectral reflectance curve which we can benefit from by calculating the difference between two bands - visible red and near-infrared. NDVI is that difference expressed as a number – ranging from -1 to 1. In a complementary way, NDRE is a metric that is used to analyse whether images obtained from multi-spectral image sensors contain healthy vegetation. It uses the ratio of Near-Infrared and the edge of Red. In the Supplementary information file, Figure S1 (Supplementary Information file, SI) displays an example of grayscale intensity corresponding to the specific NDVI and NDRE values for two different sectors in the farm. Then, the whole data were rescaled using StandardScaler method, adjusting values to the standard normal distribution with a mean of 0 and a standard deviation of 1. Sentinel satellite images are provided every 5 days. The spatial resolution of Sentinel imagery, pixel, is approximately  $10 \times 10$ m, which closely corresponds to the typical canopy size of an individual avocado tree. The closest available image of each harvest day was used for the model. The dataset, including NDVI and NDRE features, was constructed by averaging data from both harvest sectors for each corresponding harvest date.

# 2.4. Reference data: dry matter determination

Dry matter content was used as the reference parameter for ripeness assessment. Its determination was performed following the procedure described below. Every avocado was peeled, and three slices weighing about 4–5 g in total were obtained from each fruit, ensuring that each sample included both mesocarp and endocarp sections. The slices were placed on a watch glass and weighted using a Boeco scale model BWL 51 (Boeckel & Co. GmbH & Co. KG, Hamburg, Germany) with a sensibility of 0.01 g. The samples, together with the watch glass, were placed inside a LG Electronics model MH6883BAK microwaves (Seoul, South Korea) and subjected to drying for 12 min at 540 W, alongside a glass full of water to prevent sample overheating. During this process, the avocado samples lost their water content, yielding dry samples. When the program is over, the dry sample was introduced in a desiccator for 5 min to equilibrate temperature before final weighting. The dry matter percentage, DM, was calculated according to Eq. (1):

$$DM \text{ (\%)} = 100 \cdot \frac{Dry \text{ sample Weight}}{Sample \text{ weight}}$$
 (1)

# 2.5. Data engineering

The dataset includes spectral information, measurements collected by environmental sensors installed in the avocado plantation, as well as processed satellite images for calculating relevant vegetation indices. These combined datasets provide a comprehensive insight into the conditions and characteristics of the avocados under study, as detailed below.

Multispectral information was collected for a total of 476 avocados. As mentioned, three measurements were taken for each of the 4 sides of the avocado (avocado faces), giving a total of up to 12 measurements per avocado and a total of 5712 instances. Following data analysis, outliers were identified as observations lying more than 2.5 standard deviations from the mean and were subsequently removed, leaving for further processing a total of 436 avocados and 5134 entries. Each entry consists of 40 variables, encompassing measurements for red, green, blue, and infrared from various LED wavelengths: 'white\_r', 'white\_g', 'white\_b', 'white\_ir', '405\_r', '405\_g', '405\_b', '405\_ir', '455\_r', '455\_g', '455\_b', '455\_ir', '515\_r', '515\_g', '515\_b', '515\_ir', '555\_r', '555\_g', '555\_b, '555\_ir', '610\_r', '610\_g', '610\_b', '610\_ir', '655\_r', '655\_g', '655\_b', '655\_ir', '700\_r', '700\_g', '700\_b', '700\_ir', '830\_r', '830\_g', '830\_b',

'830\_ir', '890\_r', '890\_g', '890\_b', '890\_ir'. Then, each entry was also individually normalised. To do that, the StandardScaler standardization technique was used. This method adjusts each variable to have a mean of zero and a standard deviation of one across the entire data set. This ensures that all variables are on a comparable scale and prevents variables with larger value ranges from dominating.

A variable was generated specifically for the classification models, called DM\_class, which contains 3 categories of avocado ripeness: R1 (immature fruit), when the dry matter values (DM) are less than 20 %, R2 (optimal fruit for harvesting) with DM between 20 % and 23 % and, R3 (overripe fruit), when DM is higher than 23 %.

The complete study workflow is illustrated in Fig. 2, showing all the steps of the data processing from the fruit harvesting to the analysis of the model accuracies. Datasets, data preprocessing, features selection, and used machine learning models are also displayed. As explained below, the feature importance analysis (using SHAP, Shapley Additive exPlanations) was integrated into the machine learning workflow. This step, which reduced the number of features, is represented in Fig. 2 by the overlap of the 'feature importance' block with the 'machine learning' box.

# 2.6. Classification models

In the initial analysis phase, our primary objective was to formulate a solution by employing a range of classification methods on the spectral information dataset. Diverse algorithms were strategically chosen, encompassing both traditional and more advanced approaches. Notably, the lineup included well-established models such as XGBoost, Random Forest, Support Vector Classification (SVC), K-Nearest Neighbors (KNN), Adaboost, Linear Discriminant Analysis (LDA), and even Artificial Neural Networks (ANN) using a sequential model. Given the amount of data, we divided the dataset into two parts: 70 % for training and 30 % for testing. We then employed the GroupKFold technique for cross-validation, using a k-fold value of 7. This method was selected to ensure that all data points related to the same avocado remained within a single fold, preventing data leakage between the training and testing

# 2.7. Regression models

After initial tests with classification models, further experiments were carried out to evaluate the performance of regression models. These models provide the advantage of predicting a precise dry matter value, as opposed to a categorical range, offering more detailed information to growers for harvesting avocados at their optimal ripeness. In addition, various data sources were incorporated into the modelling process to enhance performance. The offline model utilized only multispectral data from the prototype, making it suitable for field conditions where internet connectivity is unreliable or unavailable. The online model incorporated additional data sources, including satellite-derived indices (NDVI and NDRE) and on-farm sensor data, allowing for a richer set of features related to avocado maturity but requiring internet access for real-time data integration.

The neural network architecture of the online model incorporates multiple input branches, each tailored to process specific types of data. A gated recurrent unit (GRU) layer is responsible for processing sensor data, while convolutional layers with max-pooling handle satellite-derived NDVI and NDRE data. The multispectral data from the prototype is processed using fully connected layers with dropout to mitigate overfitting. After each branch processes its respective data, their outputs are concatenated and passed through additional dense layers with dropout for comprehensive feature extraction. The model was compiled and trained using the Adam optimizer. More details about the obtained model, using all the available data sources, can be found in Figure S2 in the Supplementary Information file.

The dataset was split into training and testing sets using the

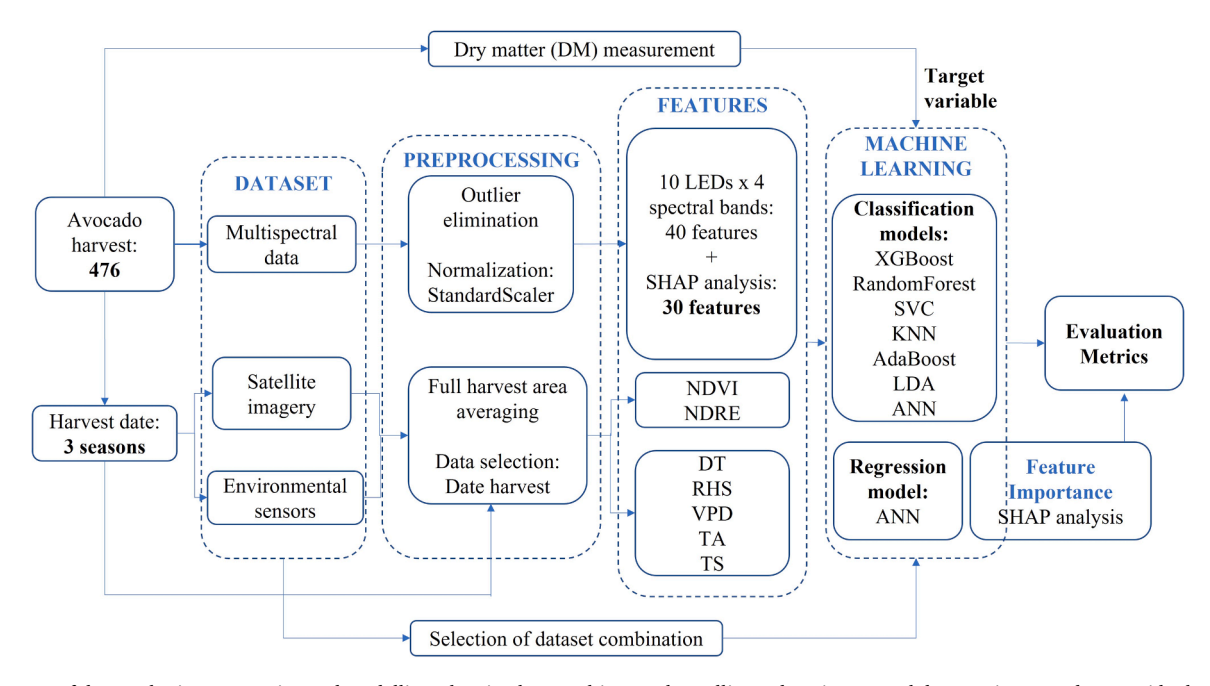


Fig. 2. Diagram of data gathering. processing and modelling, showing how multispectral, satellite and environmental data are integrated to provide the dry matter content (DM) predictions at each avocado harvest date. Features and applied machine learning models (read sections above and below for meaning of the acronyms) are also pointed out. The 'feature importance' block overlaps with the 'machine learning' box to illustrate that SHAP analysis was used to reduce the number of features.

GroupKFold cross-validation strategy, ensuring that the same groups were not present in both sets. During training, the Mean Squared Error (MSE) was employed as the loss function. The model was trained with 5-fold cross-validation, where a separate model was trained for each fold. Early stopping was applied with a patience of 30 epochs to avoid overfitting, and the best-performing model for each fold was saved based on the lowest validation loss. Hyperparameter tuning was conducted using Bayesian Optimization through the Keras Tuner library. The optimization search included the number of units in the GRU layer, the filters in the convolutional layers, and the units in the fully connected layers. A total of 10 trials were performed, and the model with the best validation loss was selected.

After training, the model's performance was evaluated on the test set. The  $R^2$  metric (coefficient of determination) was used to assess the accuracy of predictions compared to actual values. Final model performance was reported as the mean MSE across all folds, accompanied by  $R^2$  scores and graphical results. To evaluate the importance of the various data sources, different models were trained using combinations of inputs. These combinations allowed us to analyse the contributions of each data source to the predictive performance of the proposed multimodal scheme. The different combinations of input data used for model training are detailed in Table 2, where it has been indicated which information has been included as training data from three possible datasets for each particular regression model.

To reduce the complexity of the multispectral data captured by the prototype, which measures 40 spectral variables, the interpretability technique SHAP was applied to the offline model. This method, commonly used to explain complex models like neural networks, facilitated the assessment of the contribution of each wavelength to the

**Table 2**Offline and online regression models, showing the different combinations of datasets used for model training.

Data sources	Online					Offline	
Satellite data	/	1	1		1		
Environmental data	•	1		1		1	
Multispectral data	•		•	•			✓

model's predictions [41]. The SHAP analysis was performed on the best-performing offline model, trained exclusively with the spectral variables. By using SHAP, the most relevant spectral bands were identified, which enabled a potential reduction in the number of LEDs required in the prototype. This approach not only simplifies the hardware design but also enhances the data processing pipeline by eliminating redundant or less informative features. The insights gained from these techniques informed decisions to streamline the prototype, thereby improving both its efficiency and cost-effectiveness.

#### 3. Results

## 3.1. Exploratory data analysis

In this section, we present an exploratory analysis of the collected data to gain insights into the characteristics and distributions of key variables. The dry matter content, which is the variable to be predicted by the models developed in this study, had a mean of 21.59 %, ranging from a minimum of 12.20 % to a maximum of 32.50 % (as illustrated by the density plot distribution, Fig. 3A).

During the first harvest (2020–2021), a relatively small number of avocados with low dry matter content (R1) were collected. In response, efforts were made during the second harvest to increase the proportion of avocados within this lower DM category. This intentional adjustment in harvesting strategy is reflected in the observed differences between the first and second harvest periods. Specifically, the second harvest shows a more pronounced peak in the lower DM range, indicating a successful increase in the collection of avocados with the desired lower moisture content (Fig. 4A).

The correlations between spectral variables and dry matter content were examined. This analysis aimed to understand the relationship between avocado spectral characteristics and their dry matter content, essential for accurate predictive modelling. The correlation analysis of the variables reveals that certain variables are highly correlated with each other, as it can be derived from heatmap shown Figure S3 in the Supplementary Information file. This redundancy in the features can lead to overfitting in the models, and, in addition, to increasing their

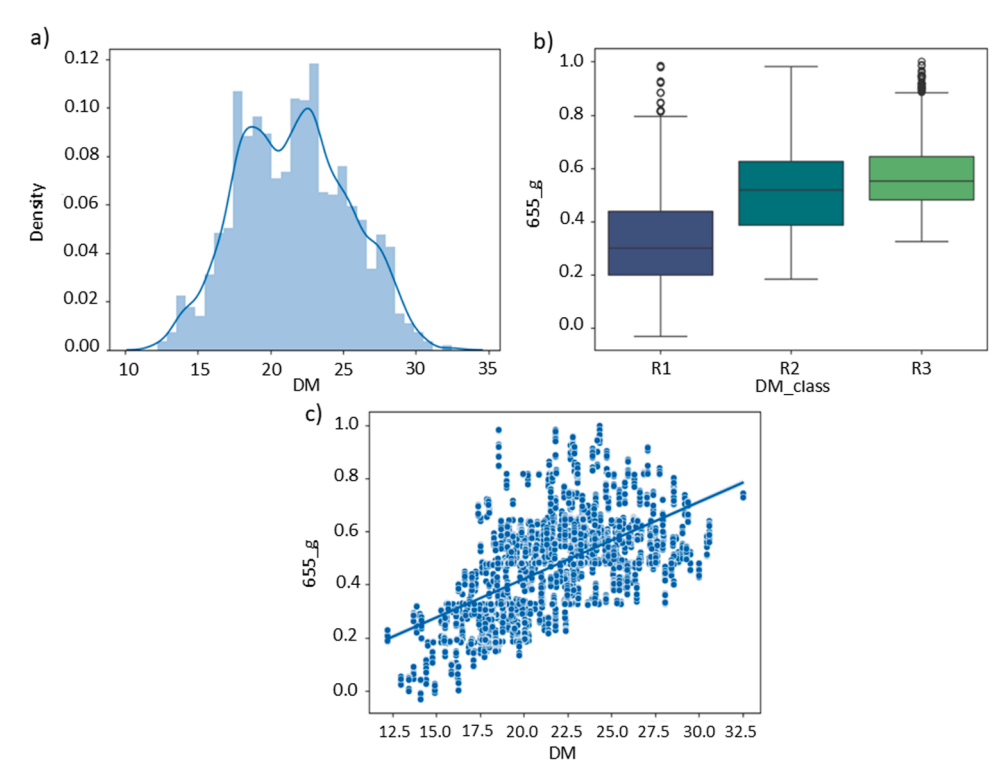


**Fig. 3.** Distribution and correlation of dry matter content (DM) and the spectral variable 655\_g across all collected data. A) Density plot showing the overall distribution of DM values. B) Boxplot illustrating the distribution of 655\_g across different DM classes (R1, R2, R3). C) Scatterplot demonstrating the positive correlation between DM and 655\_g.

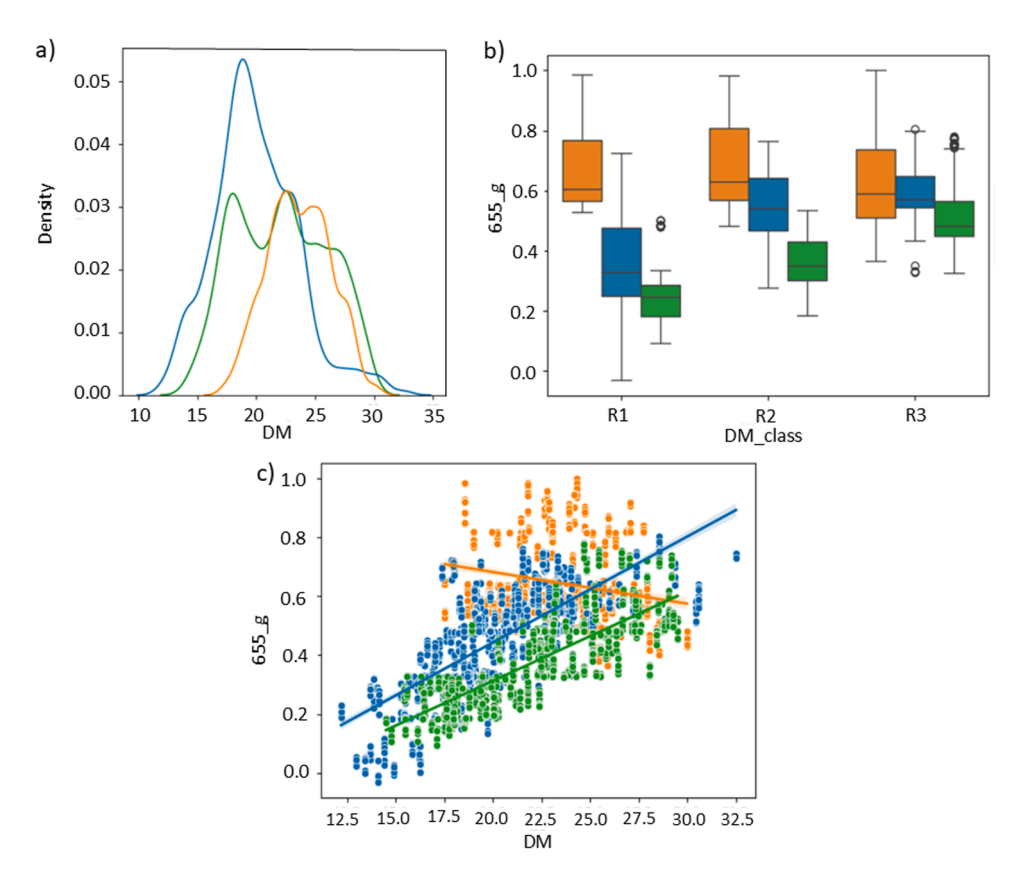


**Fig. 4.** Distribution and correlation of dry matter content (DM) and the spectral variable 655\_g separated by harvest periods. (A) Density plot showing the distribution of DM values across different harvest periods. (B) Boxplot displaying the distribution of 655\_g across DM classes (R1, R2, R3) for each harvest period (orange, harvest period 1; blue, harvest period 2; and, green, harvest period 3). (C) Scatterplot highlighting the correlation between DM and 655\_g within each harvest period.

computational complexity. Therefore, feature reduction could be beneficial for enhancing the model's efficiency and preventing information redundancy, while still maintaining the predictive capacity of the models. Thus, according to the heatmap, the variables most strongly correlated with dry matter content originate from the LEDs 610, 655, 700, and 890 nm (all above 0.5). This positive correlation among the LED values is evident in the scatter plots and boxplots corresponding to each of the classes. Specifically, the boxplot (Fig. 4B) shows the distribution of 655\_g across different harvest periods (R1, R2, R3), and the scatterplot (Fig. 4C) highlights the positive correlation between 655\_g and DM. This correlation becomes stronger as the avocados ripen, indicating that 655\_g is a reliable predictor of DM. When analysing the data separated by harvest period, the general trend of increasing 655\_g with higher DM is consistent across the full dataset; however, this trend is less evident during the first harvest, likely due to the scarcity of avocados with lower DM in that period. In contrast, the correlation between 655 g and DM becomes more apparent in the second and third harvests. This enhanced correlation in the later harvests is likely a result of the adjustments made to the harvesting strategy after the first period, which aimed to increase the collection of avocados with lower DM.

# 3.2. Results of classification models (offline model)

The evaluation of classification models for predicting avocado maturity stages, including R1, R2, and R3 using spectral measurements obtained from a multispectral prototype is shown in Table 3. It summarizes the average performance metrics across seven-fold cross-validation for each model. Among the models evaluated, the Artificial Neural Network (ANN) demonstrated the highest accuracy (0.74) and recall (0.96) for predicting the R3 class. However, it showed comparatively lower recall (0.37) for the R2 class. The results reveal a variation in model performance for each avocado maturity category. Specifically, we observed that the R1 and R3 categories are recognized with higher precision and recall compared to the R2 category.

# 3.3. Results of regression models

Following the classification model results, it was observed that two of the classes (R1 and R3), which represent the most distinct stages of ripeness, were well differentiated. However, the intermediate class (R2) was not as effectively separated. Given these findings, we decided to further investigate the precision of regression models, which offer a more granular approach by predicting the exact dry matter content (DM) for each avocado. Given that the best results in classification were achieved using Artificial Neural Networks (ANNs), we extended this approach to the regression models as well. Table 4 summarizes the performance of the regression models using all the combinations of the three different data sources: sensor data, satellite data, and multispectral data. The checkmarks (1) indicate the data source that has been included in the regression models. All models have demonstrated high predictive accuracy, as indicated by the R<sup>2</sup> coefficient of determination, which ranges from 0.81 to 0.91. The online model achieved the highest coefficient (0.91), suggesting a marginally better performance

**Table 3** Performance of classification models.

Model	Accuracy	Recall			Precision		
		R1	R2	R3	R1	R2	R3
XGBoost	0.68	0.80	0.41	0.77	0.79	0.45	0.71
RandomForest	0.68	0.80	0.40	0.76	0.79	0.46	0.70
SVC	0.67	0.80	0.40	0.74	0.77	0.46	0.69
KNN	0.64	0.76	0.44	0.67	0.74	0.42	0.71
AdaBoost	0.60	0.62	0.41	0.72	0.75	0.36	0.67
LDA	0.66	0.77	0.44	0.72	0.79	0.45	0.69
ANN	0.74	0.81	0.37	0.96	0.90	0.63	0.68

compared to the offline model. Standard deviation (sd) values were consistently low across all models and data sources, with the online model exhibiting slightly better precision (e.g., sd =0.015 compared to sd =0.028 for the offline model). These results indicate robust and reliable predictions, with minimal variability.

#### 3.4. Spectral feature relevance

Fig. 5 presents the SHAP analysis applied to the predictive model for determining dry matter in avocados. The plot highlights the 20 most relevant spectral features, ranked by their contribution to the model's predictions while the SHAP values for the 40 features are included in Table S1. Each dot represents a sample, and its position along the x-axis indicates the SHAP value, i.e., the impact of that specific feature on the model's output. The colour gradient represents the feature value, with blue indicating lower values and pink higher values.

The results reveal that the spectral bands around 700 nm (700\_r and 700\_g), 455 nm (455\_r and 455\_b), and 405 nm (405\_r, 405\_b, and 405\_g) show the highest contributions to the model's predictions, underscoring their importance for capturing relevant information. In contrast, certain bands, such as those at 555 nm, exhibit negligible contributions, suggesting they could be excluded without significantly affecting the model's performance.

To evaluate the impact of dimensionality reduction, the model was retrained using only the top 30 features identified by the SHAP analysis. Notably, this reduced model maintained the same performance metrics as the original model trained with all 40 features, demonstrating that the less relevant spectral bands do not provide additional predictive power. This finding supports the hypothesis that the number of LEDs in the prototype can be reduced, simplifying the hardware design and optimizing the data acquisition pipeline while preserving accuracy and robustness.

#### 4. Discussion

The development of predictive models for avocado ripeness, based on multispectral data, satellite imagery, and environmental sensor data, holds significant potential for optimizing harvest timing and enhancing quality control processes in avocado production. This study provides valuable insights into the relationship between dry matter content (DM), a key indicator of avocado ripeness, and various environmental and spectral variables, ultimately supporting more informed decisionmaking in agriculture. However, several aspects warrant further consideration to refine and enhance these models.

# 4.1. Challenges in classification models

Initially, classification models were employed to categorize avocados into three ripeness stages: immature (R1), intermediate (R2), and overripe (R3). While these models performed well in distinguishing the extreme stages (R1 and R3), they faced challenges in accurately classifying the intermediate stage (R2). This stage exhibited reduced precision and recall, likely due to the gradual transition between ripeness stages, which is difficult to define within the dataset. These limitations highlight the inherent complexity of using discrete categories to represent what is essentially a continuous biological process.

## 4.2. Regression models: improved accuracy and insights

Given the challenges with classification models, regression models were employed to predict DM as a continuous variable. These models demonstrated superior performance, likely due to their ability to leverage continuous data from multiple sources, rather than discrete classifications as previously reported [28]. The results highlighted the significant improvements achieved by integrating spectral, environmental, and satellite-based indices, further emphasizing the value of a

**Table 4**Results of offline and online regression models, showing the different combinations of datasets used for model training.

Data sources	Online						Offline
Satellite data	<b>✓</b>	<b>✓</b>	<b>✓</b>		<b>✓</b>		
Environmental data	✓	✓		✓		✓	
Spectral data	✓		✓	✓			✓
$R^2$	0.86	0.91	0.86	0.85	0.90	0.82	0.81
sd / RMSE	0.028	0.015	0.030	0.026	0.020	0.033	0.032



Fig. 5. SHAP analysis of the 20 most important spectral features contributing to the predictive model for avocado DM content. The x-axis represents SHAP values (feature impact on model output), and the y-axis lists the spectral features ranked by relevance. Each dot corresponds to a sample, with the colour indicating the feature value (blue: low, pink: high). This analysis identified the key wavelengths contributing to the predictions, enabling the potential elimination of redundant features.

comprehensive data-driven approach. An interesting observation was the variability in model performance depending on the data sources used. Although all data types contributed to better DM predictions, differences in  $\mathbb{R}^2$  values between models using satellite indices and those using environmental sensors suggest that the architecture and integration methodology of the models could influence their effectiveness.

The SHAP analysis provides valuable insights into the contribution of

individual spectral bands to the model's performance, facilitating the identification of the most informative wavelengths for predicting dry matter in avocados. The results demonstrate that spectral bands around 700 nm, 455 nm, and 405 nm consistently exhibit high importance, while others, such as the 555 nm band, contribute minimally. This suggests that certain wavelengths are redundant or less informative, and their removal could simplify the hardware setup without compromising

predictive accuracy. Furthermore, our investigation revealed substantial redundancy among spectral features, as evidenced by high correlations between certain bands. This redundancy indicates that several features capture overlapping information, which not only increases the complexity of the data processing pipeline but also limits the interpretability of the model. By eliminating less relevant or redundant wavelengths, we can streamline the spectral acquisition process, reduce computational demands, and optimize hardware design.

Notably, retraining the model with the top 30 features, identified by SHAP as the most relevant, maintained the same predictive performance as the model trained with all 40 spectral bands. This underscores that the excluded bands do not add significant information to the model. Such dimensionality reduction not only confirms the robustness of the SHAPbased feature selection approach but also highlights the potential for cost and efficiency improvements in the multispectral prototype. These findings are consistent with prior studies demonstrating that carefully selected subsets of spectral bands can achieve comparable or even superior performance to models trained on the full spectrum. By focusing on the most relevant bands, it is possible to design simpler and more cost-effective devices, which are particularly advantageous for portable or field-based applications. Future work could further explore the integration of feature selection with hardware design, ensuring that both the computational and physical components of the system are optimized for real-world deployment.

# 4.3. Strengths of the multimodal sensing approach

A key contribution of this study is the integration of multispectral data with environmental sensor data and satellite-derived vegetation indices (e.g., NDVI, NDRE). This multimodal approach provides a holistic understanding of avocado ripeness by combining physical characteristics (e.g., spectral reflectance) with environmental factors. This synergy significantly enhances the predictive accuracy of the models compared to relying on any single data source [40]. For example, regression models that incorporated both multispectral data and satellite indices achieved an impressive R<sup>2</sup> of 0.91, demonstrating a robust predictive capability. Importantly, both satellite data and sensor data, when analysed independently, were shown to be highly effective in predicting DM, underscoring the importance of these sources in precision agriculture.

# 4.4. Limitations and future work

Despite the promising results, there are opportunities to further enhance these predictive models. One key recommendation is to expand the dataset to include data from multiple harvest seasons. Incorporating data from diverse growing conditions, climatic variations, and different crop cycles can enrich the models, making them more generalizable and robust across varied contexts. Additionally, future efforts could explore improvements in model architectures to better capture the complex relationships between multispectral, environmental, and satellite data. Advanced techniques, such as deep learning models or hybrid approaches, may offer improved predictive capabilities by effectively managing the heterogeneity and scale of the input data.

# 5. Conclusions

This study highlights the potential of integrating multispectral, satellite, and environmental data to develop accurate predictive models for estimation of avocado ripeness stage. The results emphasize the value of multimodal sensing data and continuous prediction frameworks in optimizing harvest strategies. By addressing the challenges identified, such as classification ambiguity, and by pursuing future directions involving expanded datasets and advanced model architectures, these predictive tools can become invaluable assets for precision agriculture, ultimately improving both productivity and sustainability in avocado

production. The models developed herein have the potential to revolutionize avocado harvesting strategies. Accurate predictions of dry matter content, which is directly correlated with fruit ripeness, are essential for ensuring that avocados are harvested at their optimal stage. By enabling growers to determine peak maturity with precision, these models can minimize losses due to overripe or underripe harvests, thereby reducing post-harvest waste and improving overall fruit quality. Furthermore, the ability to predict dry matter content in real-time and in situ, using portable multispectral systems could streamline logistics, allowing for better synchronization between harvest timing and market demand for optimal ripeness.

#### **Funding statement**

This research was partially supported by the Spanish government with projects AEI-010500–2020–52, AEI-010500–2021b-5, and AEI-010500–2022b-27 funded by the Ministry of Industry, Trade and Tourism (MINCOTUR) within the support program for AEI to contribute to improving the competitiveness of the Spanish industry, and with the support of the European Union through the Recovery, Transformation and Resilience Plan, Next Generation EU Funds of the European Union. This work also was supported by the project PID2022–138727OB-I00 funded by MCIN/AEI/10.13039/501100011033 and, by ERDF "A way of making Europe", by the "European Union", and also this work is part of the "Applied research from the UGR research and transfer plan projects" of University of Granada 2023, C.ING.170.UGR23, funded by the Consejería de Universidad, Investigación e Innovación from Junta de Andalucía and by the European Union under the FEDER Program Andalucía 2021–2027.

#### **Ethics statement**

Not applicable: This manuscript does not include human or animal research.

# CRediT authorship contribution statement

Nuria López-Ruiz: Writing - original draft, Visualization, Methodology, Funding acquisition, Formal analysis. Silvia Prieto-Sánchez: Writing - original draft, Software, Methodology, Formal analysis, Data curation. Celia E. Ramos-Lorente: Writing - review & editing, Methodology, Investigation. Alejandro Fernández-Moreno: Writing - review & editing, Methodology, Conceptualization. Antonio J. Pérez-Ávila: Writing - review & editing, Software, Methodology, Investigation. David Álvarez-León: Writing - review & editing, Software, Formal analysis, Data curation. Isabel M. Pérez de Vargas-Sansalvador: Writing – review & editing, Visualization, Methodology, Investigation. Alexander García-Cardenas: Writing – review & editing, Investigation, Conceptualization. Beatriz Molina-García: Writing – review & editing, Methodology, Investigation. Alberto J. Palma: Writing – original draft, Methodology, Investigation, Funding acquisition, Formal analysis, Conceptualization. Luis F. Capitán-Vallvey: Writing - review & editing, Methodology, Investigation, Funding acquisition, Conceptualization. Antonio Martínez-Olmos: Writing - review & editing, Supervision, Methodology, Investigation, Conceptualization. Miguel M. Erenas: Writing - review & editing, Visualization, Validation, Supervision, Conceptualization.

# Declaration of competing interest

The authors declare that they have no known competing financial interests or personal relationships that could have appeared to influence the work reported in this paper.

#### Acknowledgements

We thank Company Group La Caña S.L. (Granada, Spain) for their support in providing environmental data and harvesting avocados on their farms and those of their associated farmers.

#### Supplementary materials

Supplementary material associated with this article can be found, in the online version, at doi:10.1016/j.atech.2025.101520.

# Data availability

Data will be made available on request.

#### References

- E. Hurtado-Fernández, A. Fernández-Gutiérrez, A. Carrasco-Pancorbo, Avocado fruit— Persea americana, Exot. Fruits (2018) 37–48, https://doi.org/10.1016/ B978-0-12-803138-4.00001-0.
- [2] Food and Agriculture Organization of the United Nations. https://www.fao. org/faostat/en/#home, 2024 accessed 1 February 2025.
- [3] S. Mali, Avocado Market Report 2024, Cognitive Market Research, 2024. htt ps://www.cognitivemarketresearch.com/avocado-market-report. accessed 30 November 2024.
- [4] N. Maftoonazad, H.S. Ramaswamy, Effect of pectin-based coating on the kinetics of quality change associated with stored avocados, J. Food Process. Preserv. 32 (2008) 621–643, https://doi.org/10.1111/j.1745-4549.2008.00203.x.
- [5] U. Flitsanov, A. Mizrach, A. Liberzon, M. Akerman, G. Zauberman, Measurement of avocado softening at various temperatures using ultrasound, Postharvest Biol. Technol. 20 (2000) 279–286, https://doi.org/10.1016/S0925-5214(00)00138-1.
- [6] K.A. Cox, T.K. McGhie, A. White, A.B. Woolf, Skin colour and pigment changes during ripening of 'Hass' avocado fruit, Postharvest Biol. Technol. 31 (2004) 287–294, https://doi.org/10.1016/j.postharvbio.2003.09.008.
- [7] S.K. Lee, R.E. Young, P.M. Schiffman, C.W. Coggins, Maturity Studies of Avocado Fruit Based on Picking Dates and Dry Weight, J. Am. Soc. Hortic. Sci. 108 (1983) 390–394, https://doi.org/10.21273/JASHS.108.3.390.
- [8] A.A. Kader, Maturity, Ripening, And Quality Relationships Of Fruit-Vegetables, Acta Hortic. (1996) 249–256, https://doi.org/10.17660/ActaHortic.1996.434.30.
- [9] A. Woolf, C. Clark, E. Terander, V. Phetsomphou, R. Hofshi, M.L. Arpaia, D. Boreham, M. Wong, A. White, Measuring avocado maturity; ongoing developments, The Orchardist (2003) 40–45.
- [10] A. Mizrach, Ultrasonic technology for quality evaluation of fresh fruit and vegetables in pre- and postharvest processes, Postharvest Biol. Technol. 48 (2008) 315–330, https://doi.org/10.1016/j.postharvbio.2007.10.018.
- [11] A. White, A.B. Woolf, R. Harker, M. Davy, Measuring avocado firmness: assessment of various methods, Chapingo Ser. Hortic. 5 (1999) 389–392.
- [12] J.S. Köhne, S. Kremer-Köhne, S.H. Gay, Non-destructive avocado fruit firmness measurement, South Afr. avocado grow, Assoc. Yearb. 21 (1998) 19–21.
- [13] A.B. Woolf, R. Wibisono, J. Farr, I. Hallett, L. Richter, I. Oey, M. Wohlers, J. Zhou, G.C. Fletcher, C. Requejo-Jackman, Effect of high pressure processing on avocado slices, Innov. Food Sci. Emerg. Technol. 18 (2013) 65–73, https://doi.org/10.1016/j.jject.2013.00.011.
- [14] M.L.A.T.M. Hertog, S.E. Nicholson, K. Whitmore, The effect of modified atmospheres on the rate of quality change in 'Hass' avocado, Postharvest Biol. Technol. 29 (2003) 41–53, https://doi.org/10.1016/S0925-5214(02)00211-9.
- [15] A. Mizrach, Determination of avocado and mango fruit properties by ultrasonic technique, Ultrasonics 38 (2000) 717–722, https://doi.org/10.1016/S0041-624X (99)00154-7
- [16] C.-J. Du, D.-W. Sun, Recent developments in the applications of image processing techniques for food quality evaluation, Trends Food Sci. Technol. 15 (2004) 230–249, https://doi.org/10.1016/j.tifs.2003.10.006.
- [17] J. Pinto, H. Rueda-Chacón, H. Arguello, Classification of Hass avocado (persea americana mill) in terms of its ripening via hyperspectral images, TecnoLógicas 22 (2019) 109–128, https://doi.org/10.22430/22565337.1232.
- [18] G.D. Martins, L.C. Sousa Santos, G.J. Dos Santos Carmo, O.F. Da Silva Neto, R. Castoldi, A.I.M.R. Machado, H.C. De Oliveira Charlo, Multispectral images for estimating morphophysiological and nutritional parameters in cabbage seedlings, Smart Agric. Technol. 4 (2023) 100211, https://doi.org/10.1016/j. atech.2023.100211.
- [19] I. Arzate-Vázquez, J.J. Chanona-Pérez, M. de J. Perea-Flores, G. Calderón-Domínguez, M.A. Moreno-Armendáriz, H. Calvo, S. Godoy-Calderón, R. Quevedo, G. Gutiérrez-López, Image Processing Applied to Classification of Avocado Variety Hass (Persea americana Mill.) During the Ripening Process, Food Bioprocess Technol. 4 (2011) 1307–1313, https://doi.org/10.1007/s11947-011-0595-6.

- [20] X. Lin, H. Zhang, L. Hu, G. Zhao, S. Svanberg, K. Svanberg, Ripening of avocado fruits studied by spectroscopic techniques, J. Biophotonics 13 (2020) e202000076, https://doi.org/10.1002/jbio.202000076.
- [21] Z. Wei, W. Fang, UV-NDVI for real-time crop health monitoring in vertical farms, Smart Agric. Technol. 8 (2024) 100462, https://doi.org/10.1016/j. atech.2024.100462.
- [22] B.-H. Cho, K. Koyama, E. Olivares Díaz, S. Koseki, Determination of "Hass" avocado ripeness during storage based on smartphone image and machine learning model, Food Bioprocess Technol. 13 (2020) 1579–1587, https://doi.org/10.1007/s11947-020-02494-x.
- [23] O.O. Olarewaju, I. Bertling, L.S. Magwaza, Non-destructive evaluation of avocado fruit maturity using near infrared spectroscopy and PLS regression models, Sci. Hortic. 199 (2016) 229–236, https://doi.org/10.1016/j.scienta.2015.12.047.
- [24] S. Sohaib Ali Shah, A. Zeb, W.S. Qureshi, M. Arslan, A. Ullah Malik, W. Alasmary, E. Alanazi, Towards fruit maturity estimation using NIR spectroscopy, Infrared Phys. Technol. 111 (2020) 103479, https://doi.org/10.1016/j. infrared.2020.103479.
- [25] R.J. Blakey, Evaluation of avocado fruit maturity with a portable near-infrared spectrometer, Postharvest Biol. Technol. 121 (2016) 101–105, https://doi.org/ 10.1016/j.postharvbio.2016.06.016.
- [26] M. Noguera, B. Millan, J.M. Andújar, Low-Cost New, Hand-held multispectral device for In-field fruit-ripening assessment, Agriculture 13 (2022) 4, https://doi. org/10.3390/agriculture13010004.
- [27] D. Pineda, J. Pérez, D. Gaviria, K. Ospino-Villalba, O. Camargo, MEDUSA: an open-source and webcam based multispectral imaging system, HardwareX 11 (2022) e00282, https://doi.org/10.1016/j.ohx.2022.e00282.
- [28] L.S. Magwaza, S.Z. Tesfay, A review of destructive and non-destructive methods for determining avocado fruit maturity, Food Bioprocess Technol. 8 (2015) 1995–2011, https://doi.org/10.1007/s11947-015-1568-y.
- [29] H. Zheng, H. Lu, A least-squares support vector machine (LS-SVM) based on fractal analysis and CIELab parameters for the detection of browning degree on mango (Mangifera indica L.), Comput. Electron. Agric. 83 (2012) 47–51, https://doi.org/ 10.1016/j.compag.2012.01.012.
- [30] N. El-Bendary, E. El Hariri, A.E. Hassanien, A. Badr, Using machine learning techniques for evaluating tomato ripeness, Expert Syst. Appl. 42 (2015) 1892–1905. https://doi.org/10.1016/j.eswa.2014.09.057.
- [31] M. Zhang, M. Shen, H. Li, B. Zhang, Z. Zhang, P. Quan, X. Ren, L. Xing, J. Zhao, Modification of the effect of maturity variation on nondestructive detection of apple quality based on the compensation model, Spectrochim. Acta. A. Mol. Biomol. Spectrosc. 267 (2022) 120598, https://doi.org/10.1016/j. saa 2021 120598
- [32] M. Zhang, M. Shen, Y. Pu, H. Li, B. Zhang, Z. Zhang, X. Ren, J. Zhao, Rapid identification of apple maturity based on multispectral sensor combined with spectral shape features, Horticulturae 8 (2022) 361, https://doi.org/10.3390/ horticulturae8050361.
- [33] Y.J. Davur, W. Kämper, K. Khoshelham, S.J. Trueman, S.H. Bai, Estimating the ripeness of hass avocado fruit using deep learning with hyperspectral imaging, Horticulturae 9 (2023) 599, https://doi.org/10.3390/horticulturae9050599.
- [34] D. Barhate, S. Pathak, B.K. Singh, A. Jain, A.K. Dubey, A systematic review of machine learning and deep learning approaches in plant species detection, Smart Agric. Technol. 9 (2024) 100605, https://doi.org/10.1016/j.atech.2024.100605.
- [35] B.A. Torgbor, P. Sinha, M.M. Rahman, A. Robson, J. Brinkhoff, L.A. Suarez, Exploring the relationship between very-high-resolution satellite imagery data and fruit count for predicting mango yield at multiple scales, Remote Sens 16 (2024) 4170, https://doi.org/10.3390/rs16224170.
- [36] A. Robson, M. Rahman, J. Muir, Using worldview satellite imagery to map yield in avocado (Persea americana): a case study in bundaberg, Australia, Remote Sens 9 (2017) 1223. https://doi.org/10.3390/rs9121223.
- [37] J. Brinkhoff, B.W. Dunn, T. Dunn, A. Schultz, J. Hart, Forecasting field rice grain moisture content using Sentinel-2 and weather data, Precis. Agric. 26 (1) (2025), https://doi.org/10.1007/s11119-025-10228-2.
- [38] P. Karmakar, S.W. Teng, M. Murshed, S. Pang, Y. Li, H. Lin, Crop monitoring by multimodal remote sensing: a review, Remote Sens. Appl. Soc. Environ. 33 (2024) 101093, https://doi.org/10.1016/j.rsase.2023.101093.
- [39] M. Der Yang, Y.C. Hsu, W.C. Tseng, H.H. Tseng, M.H. Lai, Precision assessment of rice grain moisture content using UAV multispectral imagery and machine learning, Comput. Electron. Agric. 230 (2025) 109813, https://doi.org/10.1016/j. compag.2024.109813.
- [40] A. Martínez-Olmos, P.M. Olmos, M.M. Erenas, P. Escobedo, Portable multispectral system based on color detector for the analysis of homogeneous surfaces, J. Sens. 2019 (2019) 1–8, https://doi.org/10.1155/2019/1519753.
- [41] R. John Martin, R. Mittal, V. Malik, F. Jeribi, S.Tabrez Siddiqui, M. Alamgir Hossain, S.L. Swapna, XAI-Powered smart agriculture framework for enhancing food productivity and sustainability, IEEE Access 12 (2024) 168412–168427, https://doi.org/10.1109/ACCESS.2024.3492973.
- [42] P. Escobedo, C.E. Ramos-Lorente, A. Ejaz, M.M. Erenas, A. Martínez-Olmos, M. A. Carvajal, C. García-Núñez, I. de Orbe-Payá, L.F. Capitán-Vallvey, A.J. Palma, QRsens: dual-purpose quick response code with built-in colorimetric sensors, Sensors Actuators B Chem 376 (2023) 133001, https://doi.org/10.1016/j.cpb/2022.132001